

BBA 41354

INVESTIGATION OF BACTERIORHODOPSIN-INTERMEDIATE RELAXATION BY MEANS OF TEMPERATURE PULSE

B.V. ZUBOV, T.M. MURINA, A.M. PROKHOROV, N.A. SULIMOV, N.M. CHERNAVSKAYA, D.S. CHERNAVSKY and I.V. CHIZHOV

P.N. Lebedev Physical Institute of the U.S.S.R. Academy of Sciences, M.V. Lomonosov Moscow State University, Moscow (U.S.S.R.)

(Received December 13th, 1982)

(Revised manuscript received May 30th, 1983)

Key words: Bacteriorhodopsin; Temperature pulse; Electron resonance tunneling; (Kinetics)

The kinetics of bacteriorhodopsin action are investigated by means of the temperature pulse method. The temperature jump is provided by a short laser pulse (wavelengths $\lambda_1 = 2.94 \mu\text{m}$ or $\lambda_2 = 10.6 \mu\text{m}$). The kinetics of evolution of the spectral intermediates M-412 and O-640 are investigated. A very fast increase in the O-640 form is observed as a result of the temperature jump. The experimental results are most consistent with the physical model based on electron resonance tunneling and permitting two protons transported per cycle. A branched scheme of the bacteriorhodopsin photocycle and corresponding mathematical equations are discussed.

Introduction

This paper reports the results of the investigation of the photocycle of light-adapted bacteriorhodopsin assayed by means of temperature pulses created by infrared laser radiation ($\lambda_1 = 2.94 \mu\text{m}$ or $\lambda_2 = 10.6 \mu\text{m}$). The method allows the attainment in thin films of a quick temperature jump by tens of degrees and its sufficiently rapid relaxation to the initial value.

A part of the bacteriorhodopsin photocycle, which involves spectral intermediates M-412 and O-640, was investigated. The above stages of the bacteriorhodopsin cycle have recently attracted attention because, according to the data of Refs. 1–4, the branching in the bacteriorhodopsin cycle takes place at the stage of formation and relaxation of M-412. In the theoretical scheme based on electron resonance tunneling, the branching may occur after the return of the electron to the initial site by the tunneling process (state 5 in Ref. 5). The development of this scheme in detail allows

the association of the branching process with alterations of the proton quantum yield in the two-proton transport model. It was shown experimentally in Refs. 7–9 that more than one proton can be transferred during one cycle. This problem of quantum yield is likely to be solved in the stages of M and O intermediate formation. The method of pulsed heating, which has not been used before for these purposes, is in our opinion the most promising [16] for experimental investigation of the details of the above processes.

Materials and Methods

We used the technique of pulsed laser radiation heating of purple membranes (*Halobacterium halobium*) with the subsequent recording of changes in the parameters of spectral transitions in the bacteriorhodopsin photochemical cycle. A sample was placed into a special chamber which served as a thermostat in the temperature range from -196 to $+60^\circ\text{C}$. The cycle was excited by

the second harmonic of an Nd-YAG laser with $\lambda = 0.53 \mu\text{m}$, $t_{\text{gen}} = 15 \text{ ns}$ and $E_{\text{rad}} = 20 \text{ mJ/cm}^2$. A thermal pulse was generated by absorption of radiation from an Er-YAG ($\lambda = 2.94 \mu\text{m}$, $t = 150 \mu\text{s}$) and CO_2 ($\lambda = 10.6 \mu\text{m}$, $t = 1 \mu\text{s}$) laser. To prepare the samples an aqueous suspension of purple membranes was drained on quartz or BaF_2 sublayers and the film was subsequently moistened and sealed. The film thickness was $10 \pm 3 \mu\text{m}$. This sample had the same kinetics and spectral parameters as those in an aqueous suspension. At 2.94 and $10.6 \mu\text{m}$ the absorption coefficient was $0.5 \cdot 10^4$ and $0.2 \cdot 10^3 \text{ cm}^{-1}$, respectively. To determine a precise temperature regime for a sample under laser heating a nonstationary equation for heat conduction should be solved. The main difficulty here is to estimate the efficiency of heat transfer in the sublayer. Rough numerical estimates taking into account the generation time and absorption coefficient point, however, to a sufficiently uniform heating of $10\text{-}\mu\text{m}$ samples by Er and CO_2 laser irradiation.

The experimental measurement of temporal parameters of the temperature pulse for the Er laser gives a temperature rise time of $t_1 = 150 \mu\text{s}$ and a cooling half-time of $t_2 = 1\text{--}1.5 \text{ ms}$. The sample heating was varied from the minimum registered ($\Delta T \approx 5^\circ\text{C}$) up to the bacteriorhodopsin denaturation temperature by changing the energy of thermal irradiation. Such characteristics of the temperature pulse make it possible to observe the nonstationary thermal effect in millisecond- and slower relaxation processes. Spectral measurements were mainly carried out at the two wavelengths, 424 and 660 nm, where the decay of the M form and the formation and decay of the O form are most readily observed. Investigation of the temperature characteristics of the M and O intermediates for the samples used in the experiment showed good agreement between the measured values and literature data [10,11]. This refers to the values of the rate constants for formation and decay and the amplitude of the O form, as well as their temperature dependence in the range $0\text{--}60^\circ\text{C}$.

Results and Discussion

The following text lists the most important results obtained by means of thermal irradiation.

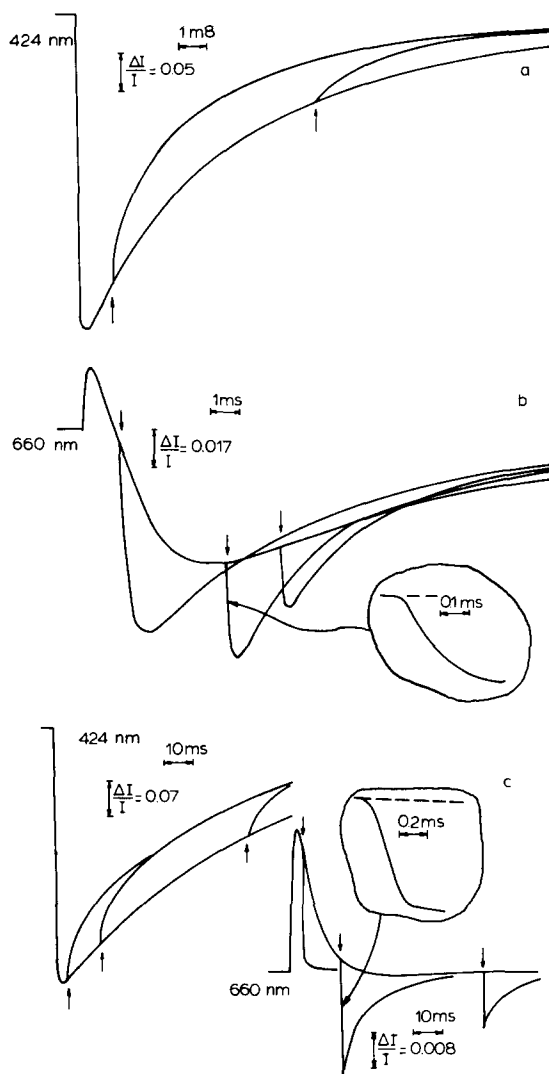


Fig. 1. Characteristic curves of the absorbance changes in the bacteriorhodopsin photocycle. The curves for different delay times of switching on of the thermal pulse are combined with the usual curve. The pointers indicate moments of switching on of the thermal pulse (experiments with Er laser). (a) $\lambda = 424 \text{ nm}$, $T = 23^\circ\text{C}$, $T_m \approx 45^\circ\text{C}$. (b) $\lambda = 660 \text{ nm}$, $T_0 = 23^\circ\text{C}$, $T_m \approx 45^\circ\text{C}$. (c) $\lambda = 424 \text{ nm}$ and $\lambda = 660 \text{ nm}$, $T_0 = 2^\circ\text{C}$, $T_m \approx 25^\circ\text{C}$.

(1) Pulsed heating of the samples increases the rate of M form decay (Fig. 1a). The maximum temperature T_m in the sample was estimated by measuring the rate constant of thermal decay. It turned out to be close to the value of T_m obtained from the energy characteristics of laser radiation.

(2) In the 660 nm region an absorption signal

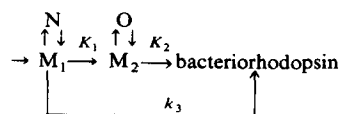
occurs as a result of the thermal pulse (see Fig. 1b and c). This signal sharply differs in its kinetic parameters from the absorption signal corresponding to the usually observed intermediate O-640 (see below). Since in the region of 570–660 nm these signals are similar in their spectral characteristics, we introduce the following notations for their distinction. We shall ascribe the absorption signal observed at the thermal pulse to a new intermediate O_2 , and intermediate O-640 to O_1 .

(3) The maximal amplitude of O_2 was observed with the thermal pulse switched on at the moment when intermediate M-412 reached its maximum value (in Fig. 1a and b this corresponds to 300 μ s). When switching on the thermal pulse in successively longer delay times the O_2 maximal amplitude decreases with a time constant close to that of the M form relaxation under stationary conditions.

(4) The characteristic half-time τ_2 for increase in the O_2 form concentration was estimated in the experiments with the CO_2 laser (the generation time is about 1 μ s). This time depends slightly on the temperature T_m . In the range $T_m = 20$ – $80^\circ C$ and at the initial temperature $T_0 = 0^\circ C$, it changes from 100 μ s up to approx. 50 μ s. In the experiments with the Er laser, the rise time of O_2 absorption was of the same order as the laser generation time ($t_{gen} = 150 \mu$ s). The O_2 absorption rise half-time $\tau_2 = 50$ – 100μ s is shorter than the time constants for formation and decay of the O-640 intermediate in the experiments without pulsed heating. For example, at $t = 10^\circ C$, $\tau_{form} \approx 7$ ms and $\tau_{dec} \approx 22$ ms; at $T = 50^\circ C$ these values are 0.4 and 0.8 ms, respectively.

(5) For the decrease in the O_2 form concentration the time constant is close to that of M form decay at pulsed heating (see Fig. 1a–c).

A set of the results obtained cannot be explained in the framework of the scheme proposed in Refs. 1–3. According to this scheme decay of the M form occurs as follows (see Scheme I):



Scheme I.

The exchanges $M_1 \rightleftharpoons N$ and $M_2 \rightleftharpoons O$ are con-

sidered to be fast with respect to K_1 , K_2 and K_3 . Moreover, the rate constant K_3 is assumed to be much smaller than K_1 and K_2 under normal conditions. For such a relationship between the constants, solution of the corresponding system of equations for the intermediate has the form:

$$M_1(t) = M_0 \gamma \exp(-qt) \quad (1)$$

$$N(t) = M_0(1 - \gamma) \exp(-qt) \quad (2)$$

$$M_2(t) = M_0 \beta q / (q - p) [\exp(-pt) - \exp(-qt)] \quad (3)$$

$$O(t) = M_0(1 - \beta) q / (q - p) [\exp(-pt) - \exp(-qt)] \quad (4)$$

$$M(t) = [M_1 + M_2](t) = M_0 [\beta q / (q - p) \exp(-pt) - [\beta q / (q - p) - \gamma] \exp(-qt)] \quad (5)$$

where M_0 is the concentration of the M form at the initial moment of time (the rate of M_1 formation is considered to be fast with respect to its relaxation rate); γ and β constants of equilibrium between M_1 and N , and M_2 and O , respectively; $q = \gamma K_1$ the rate constants of formation of M_2 and O intermediates; and $p = \beta K_2$ the rate constant of decay of these intermediates.

M_1 and M_2 are the forms considered to be spectrally close and observed as a single M intermediate, provided q and p are equal to τ_{form}^{-1} and τ_{dec}^{-1} , respectively (see above).

The scheme explains in principle the temperature dependence of the O form amplitude [13] due to the temperature change of the equilibrium constant β .

This scheme does not explain, however, the results obtained with the temperature pulse. The greatest difference takes place at low temperatures ($T_0 \approx 0^\circ C$) and not very strong heating ($T_m \leq 40^\circ C$). Indeed, according to this scheme, the amplitude of response at 660 nm to the temperature pulse (amplitude of the O_2 form) should depend considerably and nonmonotonically on the time of switching of the delay. This amplitude must be maximum at switching on of the thermal pulse at the moment close to that when M_2 and O intermediates reach a maximum value at constant temperature. For example, in Fig. 1b this moment corresponds to $t_{max} = 3$ – 4 ms. The picture observed (see Fig. 1b and c) has an absolutely different character: the amplitude of O_2 has a maximum

at a short delay time and decreases with increasing delay time (see point 3).

Furthermore, in the framework of the scheme the time constant for increasing absorption, τ_2 , must depend considerably on the delay time. Thus, at low delays $t_{\text{del}} \ll t_{\text{max}}$ the time of the front must be of the order of q^{-1} (for example, at $T_0 = 0^\circ\text{C}$ and $T_m = 20^\circ\text{C}$, $q^{-1} \approx 2$ ms). The front observed under these conditions is considerably shorter (see point 4).

A kinetic scheme has been developed in this connection, based on the physical model considered in Ref. 5. The scheme provides the opportunity of transferring two protons in one photocycle and is schematically presented in Fig. 2. Retinal is represented in Fig. 2 by the line AB, and the lines XY and X'Y' correspond to two proton-transport chains (PTC I and PTC II) in contact with the edge groups A and B of retinal (group A can be compared with the Schiff base, and group B with the β -ionon ring).

The processes in retinal (light-induced electron resonance tunneling) as well as proton transport in the proton-transport chain areas closest to the retinal caused by them are considered in Ref. 5. Comparison with the other theoretical scheme is also presented therein [14,15].

Let us consider in more detail the processes of proton transport. Fig. 3 presents the profiles of the proton free energy in the proton-transport chain for different states of the bacteriorhodopsin photocycle. The potential wells correspond to the pro-

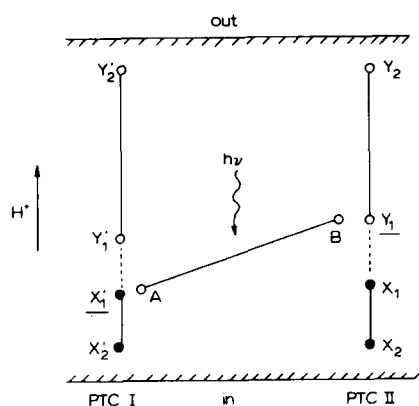


Fig. 2. Physical scheme representing two proton-transport chains (PTC I) and (PTC II) in the bacteriorhodopsin molecule. See text for explanation.

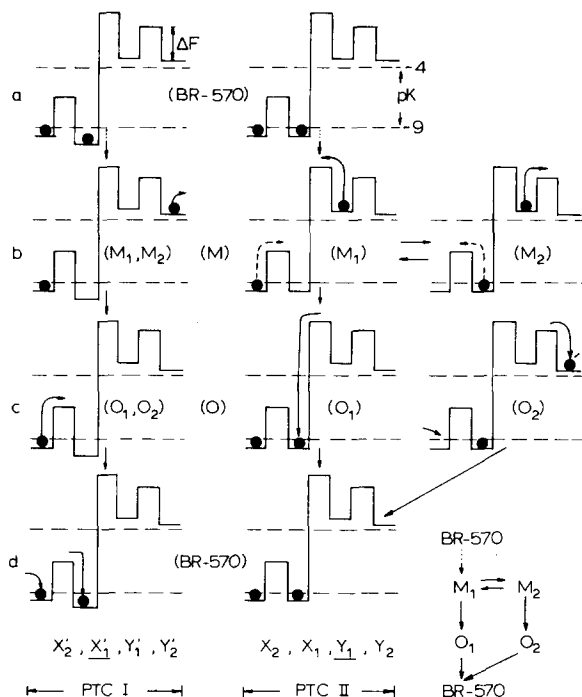


Fig. 3. Physical scheme of the energetic proton levels in proton-transport chains I and II and barriers between them in the bacteriorhodopsin photocycle. The intermediates K and L, and also barriers between groups X_2 , X'_2 , Y_2 and Y'_2 , and medium (see Ref. 5) are not indicated.

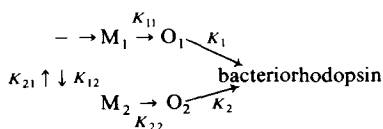
ton carriers. The levels under the lower dashed line correspond to $pK \geq 9$, those above the upper dashed line to $pK \leq 4$. Filled circles imply that the carrier is occupied by a proton; their absence implies vacancy. Fig. 3a corresponds to the initial form of BR-570 (BR, bacteriorhodopsin), Fig. 3b to the form appearing after the reverse resonance tunneling of an electron in retinal from B to A (state 5 in Ref. 5)*. The groups closest to the ends of retinal are X'_1 (deprotonated) and Y_1 (protonated). This state of bacteriorhodopsin can be identified with intermediate M.

On the right-hand side of Fig. 3b, it can be seen that there are two alternative ways for relaxation of this state: I, energized proton movement from

* The proton motion over proton-transport chain I and proton-transport chain II at the early stages of the bacteriorhodopsin photocycle is considered in detail in Ref. 6, but these stages are not essential for the problems considered in this paper.

Y_1 to Y_2 and then to the external medium; and II, the proton returning to the carrier X_1 . In the latter case the proton energy dissipates and the process in proton-transport chain II is not accompanied by proton transfer through the membrane. In this case the proton can be transferred only over proton-transport chain I, providing the quantum yield per cycle is not less than unity.

The choice of the ways of deprotonation of group Y_1 depends on the proton exchange between the carriers X_1 and X_2 , which we assume to be quick and reversible. Thus, in the scheme considered two equilibrium M forms (M_1 and M_2) and two O forms (O_1 and O_2) occur. Both M_1 and M_2 , and O_1 and O_2 must be respectively spectrally close. This follows from the fact that the spectral changes in the bacteriorhodopsin photocycle are due to the changes in charge states of proton-transport chain groups closest to the retinal. In our model these are X'_1 and Y_1 . In addition, the change of the charge state of one of these groups may influence the speed of proton transfer to the other (since it affects the electron-density distribution in the retinal). The kinetic scheme of the relaxation process of M can be presented to some approximation as follows:



Scheme II.

Scheme II contains, as in Scheme I above, six kinetic parameters. The notations correspond to the charge states presented in Fig. 3. Scheme II is described by the following system of equations:

$$dM_1/dt = -(K_{11} + K_{12})M_1 + K_{21}M_2 \quad (6)$$

$$dM_2/dt = -(K_{22} + K_{21})M_2 + K_{12}M_1 \quad (7)$$

$$dO_1/dt = -K_1O_1 + K_{11}M_1 \quad (8)$$

$$dO_2/dt = -K_2O_2 + K_{22}M_2 \quad (9)$$

At a sufficiently high rate of M_1 formation, the initial conditions have the form:

$$[M_1 + M_2](\phi) = M_0 \quad (10)$$

$$O_1(\phi) = O_2(\phi) = \phi \quad (11)$$

For the case where $K_{12}, K_{21} \gg K_{11}, K_{22}$, the solution of the system is given by:

$$M(t) = [M_1 + M_2](t) = M_0 \exp(-qt) \quad (12)$$

$$O_1(t) = M_0 q_1 / (K_1 - q) [\exp(-qt) - \exp(-K_1 t)] \quad (13)$$

$$O_2(t) = M_0 q_2 / (K_2 - q) [\exp(-qt) - \exp(-K_2 t)] \quad (14)$$

where $q = q_1 + q_2 = \alpha K_{11} + (1 - \alpha)K_{22}$ and $\alpha = K_{21}/(K_{21} + K_{12})$ is the constant of equilibrium between M_1 and M_2 forms. An essential detail of this scheme is the presence of the O_2 form spectrally close to the usual O form (in our terms, to the O_1 form), but characterized by the larger rate constant (of the order of 10^4 s^{-1}) depending slightly on temperature (see our experimental constant τ_2). Preliminary analysis has shown that the change in the O form amplitude with temperature (and of the amplitude of the absorption pulse at thermal pulse effect) can be accounted for by the different dependence of K_{11} and K_{22} on temperature, as well as by a possible change in the relative concentration of M_1 and M_2 forms (the process of exchange between M_1 and M_2 forms is assumed to be fast: greater than or equal to 10^5 s^{-1}). Due to the rate inversion in the decay chains I and II ($K_1 > q$ and $K_2 > q$) the rate constant of absorption increase at 660 nm corresponds to that of O_1 form decay in the stationary case and O_2 form decay at the thermal pulse formation. For the stationary case this coincides with the scheme suggested in Ref. 9.

We attribute the $O_2 \rightarrow$ bacteriorhodopsin relaxation to the change of charge state of X'_1 by protonation of the Schiff base (Fig. 3c). According to our assumption the latter occurs only after proton removal from group Y_1 (O_1 or O_2 forms appear) and corresponding redistribution of the electron density in retinal. If this assumption is discarded then two independent processes in proton-transport chains I and II are possible and, hence, a direct path, viz., $M \rightarrow$ bacteriorhodopsin, does not involve the O form. It was assumed in the above calculations that this process, like that of $M_1 \rightarrow O_2 \rightarrow$ bacteriorhodopsin, makes little contribution. Quantitative derivations of Scheme II do not change if we take into account the above

processes. Note also that the sequence $M_2 \rightarrow O_2 \rightarrow$ bacteriorhodopsin may imitate direct relaxation, $M \rightarrow$ bacteriorhodopsin, observed in Ref. 4, since the rate of O_2 decay is high enough and the concentration of the O_2 form under routine conditions is small. However, it manifests itself distinctly enough in our thermal pulse experiments.

In the above calculations decay of the M form was assumed to be monoexponential and, besides, possible formation of the N form was disregarded [1,2]. It is easy to see, however, that both factors can be taken into account in the framework of the physical scheme reported in Ref. 5 and this article. For example, in the case where the rates K_{12} and K_{21} are comparable with K_{11} and K_{22} , the calculation becomes a little more complicated and decay of the M form is described by two exponents. The presence of the N form may result in the same effect, if this form makes a considerable contribution in the spectral range of the M intermediate. These questions may be solved by more precise measurements.

The data obtained and their analysis indicate that the method of thermal pulse irradiated gives new and important information on the mechanism of bacteriorhodopsin functioning.

Acknowledgements

The authors wish to thank L.N. Chekulaeva who kindly provided the purple membrane preparation, and V.V. Savransky and A.K. Dyumaev for helpful discussion.

References

- 1 Lozier, R.H., Niederberger, W., Ottolenghi, M., Sivorinovsky, G. and Stoeckenius, W. (1978) in *Energetics and Structure of Halophilic Microorganisms* (Caplan, S.R. and Ginzburg, M., eds.), pp. 123–147, Elsevier/North-Holland, New-York
- 2 Ottolenghi, M. (1980) *Adv. Photochem.* 12, 97–200
- 3 Kalisky, O. and Ottolenghi, M. (1982) *Photochem. Photobiol.* 35, 109–115
- 4 Sherman, W.V., Eicke, R.R., Stafford, S.R. and Wasacz, F.M. (1979) *Photochem. Photobiol.* 30, 727–729
- 5 Chernavskaya, N.M. and Chernavsky, D.S. (1981) *Photosynthetica* 15, 195–200
- 6 Chernavsky, D.S., Djumaev, A.K., Savransky, V.V., Chernavskaya, N.M., Chizhov, I.V., Melnik, E.I., Vasiljev, G.V., Dukova, T.V. and Malina, Z.A. (1981) Preprint-163, P.N. Lebedev Institute of Physics of the Academy of Sciences in the U.S.S.R., pp. 1–26
- 7 Govindjee, R., Ebrey, T.G. and Grofts, A.R. (1980) *Biophys. J.* 30, 231
- 8 Ort, D.R. and Parson, W.W. (1979) *Biophys. J.* 25, 341–353
- 9 Kuschmitz, D. and Hess, B. (1981) *Biochemistry* 21, 5950–5957
- 10 Korenstein, R., Sherman, W.V. and Caplan, S.R. (1976) *Biophys. Struct. Mech.* 2, 267–276
- 11 Lozier, R.H. and Niederberger, W. (1977) *Fed. Proc.* 36, 1805
- 12 Gillbro, T. (1978) *Biochim. Biophys. Acta* 504, 175–186
- 13 Hoffman, W., Craca-Mignal, M., Barnard, P. and Chapman, D. (1978) *FEBS Lett.* 95, 31–34
- 14 Warshel, A. (1979) *Photochem. Photobiol.* 30, 285–290
- 15 Warshel, A. and Ottolenghi, M. (1979) *Photochem. Photobiol.* 30, 291–293
- 16 Zubov, B.V., Sulimov, N.A., Chernavskaja, N.M., Chernavsky, D.S. and Chizhov, I.V. (1982) *Biofizika (U.S.S.R.)* 27, 357–361